JOURNAL OF COLLOID AND INTERFACE SCIENCE **205,** 245–256 (1998)
ARTICLE NO. CS985687

Effect of Counterion Structure on Micellar Growth of Alkylpyridinium Surfactants in Aqueous Solution

Koos Bijma,[1] Elisabeth Rank, and Jan B. F. N. Engberts[2]

Department of Organic and Molecular Inorganic Chemistry, University of Groningen, Nijenborgh 4, 9747 AG Groningen, The Netherlands

Received October 27, 1997; accepted May 26, 1998

This paper describes the influence of counterions on the unidirectional growth of micelles formed by alkylpyridinium surfactants in aqueous solution. It is shown that the growth of spherical micelles to form wormlike micelles is strongly dependent on counterion structure. More hydrophobic counterions induce the formation of wormlike micelles at lower surfactant concentrations. Next to hydrophobicity and the type of substituent, the substitution pattern of the aromatic ring plays the most important role in micellar growth. The formation of a network of entangled, elongated wormlike micelles by alkylpyridinium surfactants with *o*-hydroxybenzoate and *p*-chlorobenzoate counterions is discussed in terms of surfactant structure. It is concluded that, next to counterion structure, the microenvironment of the counterion (substituent) in the Stern region and the structure of the surfactant monomer (i.e., the surfactant cation) play the most important role in the formation of these elongated wormlike micelles. Headgroup effects are proposed to be the main driving force for this phenomenon. © 1998 Academic Press

Key Words: **micelles; growth; NMR; alkylpyridinium surfactants; microcalorimetry; counterions.**

INTRODUCTION

Most single-chained surfactants form spherical micelles in aqueous solution at concentrations above their critical micelle concentration. Increasing the concentration of surfactant, adding salts, or adding certain characteristic organic counterions leads to the formation of wormlike micelles by unidirectional micellar growth. The presence of wormlike micelles is often reflected in an increase in relative viscosity (1). An increase in counterion binding is observed at the sphere-to-worm transitions of ionic micelles (2–4). Porte and Appell (5) computed degrees of counterion binding which are 7% higher for *n*-cetylpyridinium bromide in the cylindrical part of the aggregates than for those in the spherical part. A decrease in intermicellar interactions and a further reduction of the apolar surface area that is exposed to water are the main reasons for growth of spherical micelles. For 1-methyl-4-*n*-dodecylpyridinium iodide, an enthalpy change (6) of -0.5 kJ mol^{-1} reflects this decrease in apolar surface area that is exposed to water upon micellar growth.

Electrostatic headgroup repulsions per se can play an important role. It has been found that the tendency to grow decreases if the counterion is changed from iodide to bromide to chloride (1). This is not surprising if the degree of counterion binding for spherical micelles is taken into account. For cationic surfactants, chloride counterions have the lowest degree of counterion binding and the counterions are located further away from the micellar surface. Therefore, electrostatic headgroup repulsions are relatively large and the optimal headgroup size is large, which leads to a hampering of micellar growth. *n*-Cetyltrimethylammonium bromide forms wormlike micelles at relatively high concentrations (7, 8). Addition of electrolytes or certain organic counterions to spherical micelles also induces the formation of wormlike micelles (9, 10). In the presence of strongly binding counterions (7), such as either salicylate or *p*-chlorobenzoate, long, threadlike micelles are formed at very low concentration (around 1 m*M*), which form an entangled network. These solutions are characterized by a striking onset of viscoelasticity.

Wormlike micelles may be extremely long (many thousands of ångstroms), are rather flexible, and undergo transformations on a relatively short time scale (11). These micellar reactions consist of a forward (scission) reaction, in which the micelle spontaneously breaks at a random point along its length, and a reverse (recombination) reaction, in which one micelle combines with another.

Clausen *et al.* (12) published electron micrographs of *n*-cetyltrimethylammonium chloride/sodium chloride/sodium salicylate solutions, as a function of the salicylate concentration. Salicylate ions bind more strongly to the micellar surface than chloride ions and consequently displace them. An entangled network of long, wormlike micelles (diameter about 50 Å) is seen when sufficient salicylate is added.

The reason these micelles form extremely long, wormlike micelles is still unclear. The growth of micelles, as induced by salicylate ions, is not observed when the hydroxy group on the phenyl ring is in either the *meta* or the *para* position (7). This specificity is also found for surfactants with chlorobenzoate as the counterion, but in a reverse way.

[1] Present address: Unilever Research Laboratory, Olivier van Noortlaan 120, 3133 AT Vlaardingen, The Netherlands.

[2] To whom correspondence should be addressed.

0021-9797/98 $25.00

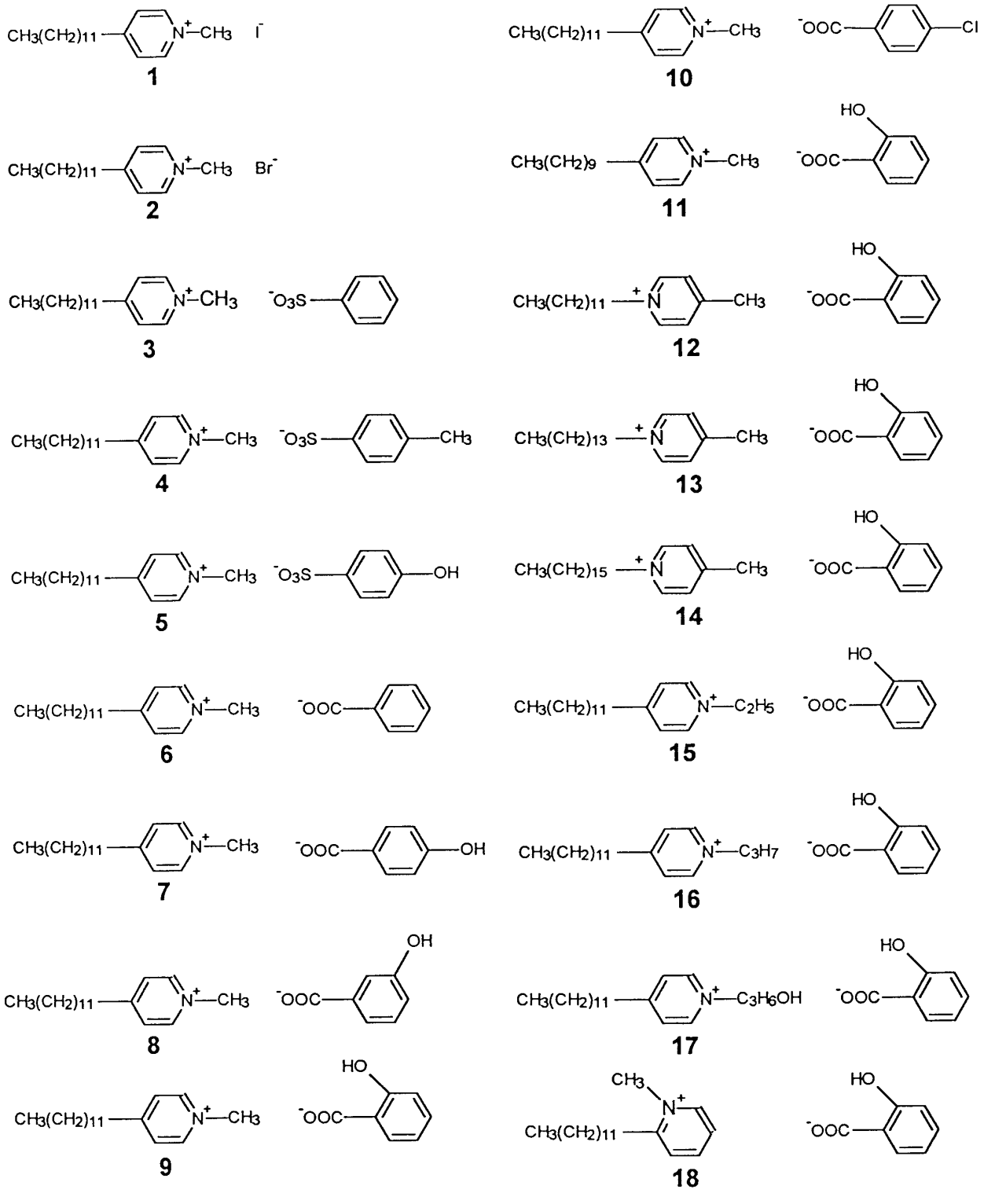

SCHEME 1

Micellar growth has been observed by light scattering (13, 14), viscosity (15, 16), flow birefringence (17), and ^{1}H NMR line broadening experiments (18). In this paper micellar growth is studied by using ^{1}H NMR spectroscopy, putting particular emphasis on the counterion type and the substitution pattern in the aromatic ring of the counterion (see Scheme 1). Several alkylpyridinium salicylate surfactants have been studied. Structural features that have been varied (see Scheme 1) in-

clude: (i) chain length of the hydrophobic moiety, (ii) headgroup size, (iii) headgroup hydrophobicity, and (iv) position of the alkyl chain in the pyridinium ring.

EXPERIMENTAL

Synthesis

The synthesis of surfactants **1** and **2** (6) and **3–9** (19) has been described previously.

The synthesis of the 1-*n*-alkyl-4-methylpyridinium bromide surfactant was performed similarly to the procedure described previously (19). The counterion exchange procedure has also been reported (19).

The synthesis of 1-alkyl-4-*n*-dodecylpyridinium bromide and 1-methyl-2-*n*-dodecylpyridinium bromide is described elsewhere (6). The salts (sodium salicylate, sodium bromide, sodium chloride, sodium *p*-chlorobenzoate, and sodium benzoate) were used as received (Aldrich).

1-Methyl-4-n-decylpyridinium Salicylate (11)

For the ^{1}H NMR ($CDCl_3$, 200 MHz), δ = 0.87 (3H, t), 1.25 (14H, b), 1.56 (2H, b), 2.66 (2H, t), 4.46 (3H, s), 6.69 (2H, m), 7.17 (1H, m), 7.55 (2H, d), 7.78 (1H, d), 8.90 (2H, d) ppm. For the ^{13}C NMR ($CDCl_3$, 200 MHz), δ = 14.1 (CH_3, 4-alkyl chain), 22.6–35.6 (CH_2, alkyl chain), 47.7 (N^+-CH_3), 116.1 (CH, counterion), 117.1 (CH, counterion), 120.0 (C, counterion), 127.5 (CH, pyridinium ring), 130.3 (CH, counterion), 132.0 (CH, counterion), 144.6 (CH, pyridinium ring), 162.1 (C, pyridinium ring), 162.7 (COH, counterion), 173.5 (COO^-, counterion) ppm.

Analysis: calculated, 74.36 %C, 9.06 %H, 3.75 %N; found, 74.35 %C, 8.95 %H, 3.77 %N.

1-n-Dodecyl-4-methylpyridinium Salicylate (12)

For the ^{1}H NMR ($CDCl_3$, 200 MHz), δ = 0.83 (3H, t), 1.13 (18H, b), 1.78 (2H, b), 2.45 (3H, s), 4.46 (2H, t), 6.64 (2H, m), 7.13 (1H, m), 7.60 (2H, d), 7.78 (1H, d), 8.77 (2H, d) ppm. For the ^{13}C NMR ($CDCl_3$, 200 MHz), δ = 14.1 (CH_3, 4-alkyl chain), 21.9 (pyr-CH_3), 22.6–31.8 (CH_2, alkyl chain), 61.3 (N^+-CH_2), 116.1 (CH, counterion), 117.0 (CH, counterion), 120.0 (C, counterion), 128.7 (CH, pyridinium ring), 130.4 (CH, counterion), 132.0 (CH, counterion), 143.6 (CH, pyridinium ring), 158.7 (C, pyridinium ring), 162.2 (COH, counterion), 173.5 (COO^-, counterion) ppm.

Analysis: calculated, 75.15 %C, 9.33 %H, 3.51 %N; found, 74.93 %C, 9.23 %H, 3.58 %N.

1-n-Tetradecyl-4-methylpyridinium Salicylate (13)

For the ^{1}H NMR ($CDCl_3$, 200 MHz), δ = 0.84 (3H, t), 1.21 (22H, b), 1.80 (2H, b), 2.48 (3H, s), 4.49 (2H, t), 6.64 (2H, m), 7.15 (1H, m), 7.62 (2H, d), 7.81 (1H, d), 8.82 (2H, d) ppm. For the ^{13}C NMR ($CDCl_3$, 200 MHz), δ = 14.1 (CH_3, 4-alkyl chain), 22.0 (pyr-CH_3), 22.6–31.8 (CH_2, alkyl chain), 61.3 (N^+-CH_2), 116.1 (CH, counterion), 117.0 (CH, counterion), 120.0 (C, counterion), 128.7 (CH, pyridinium ring), 130.4 (CH, counterion), 132.0 (CH, counterion), 143.6 (CH, pyridinium ring), 158.7 (C, pyridinium ring), 162.3 (COH, counterion), 173.6 (COO^-, counterion) ppm.

Analysis: calculated, 75.84 %C, 9.66 %H, 3.28 %N; found, 75.96 %C, 9.56 %H, 3.41 %N.

1-n-Hexadecyl-4-methylpyridinium Salicylate (14)

For the ^{1}H NMR ($CDCl_3$, 200 MHz), δ = 0.84 (3H, t), 1.22 (26H, b), 1.80 (2H, b), 2.47 (3H, s), 4.49 (2H, t), 6.66 (2H, m), 7.14 (1H, m), 7.62 (2H, d), 7.81 (1H, d), 8.81 (2H, d) ppm. For the ^{13}C NMR ($CDCl_3$, 200 MHz), δ = 14.1 (CH_3, 4-alkyl chain), 21.9 (pyr-CH_3), 22.6–31.9 (CH_2, alkyl chain), 61.3 (N^+-CH_2), 116.1 (CH, counterion), 117.0 (CH, counterion), 120.0 (C, counterion), 128.7 (CH, pyridinium ring), 130.4 (CH, counterion), 132.0 (CH, counterion), 143.6 (CH, pyridinium ring), 158.7 (C, pyridinium ring), 162.3 (COH, counterion), 173.6 (COO^-, counterion) ppm.

Analysis: calculated, 76.44 %C, 9.95 %H, 3.07 %N; found, 76.70 %C, 9.89 %H, 3.05 %N.

1-Ethyl-4-n-dodecylpyridinium Salicylate (15)

For the ^{1}H NMR ($CDCl_3$, 200 MHz), δ = 0.80 (3H, t), 1.19 (18H, b), 1.47 (5H, m), 2.65 (2H, t), 4.54 (2H, t), 6.63 (2H, m), 7.12 (1H, m), 7.55 (2H, d), 7.78 (1H, d), 8.86 (2H, d) ppm. For the ^{13}C NMR ($CDCl_3$, 200 MHz), δ = 14.0 (CH_3, 4-alkyl chain), 16.6 (CH_3, 1-alkyl chain), 22.6–35.7 (CH_2, alkyl chain), 56.5 (N^+-CH_2), 116.1 (CH, counterion), 117.1 (CH, counterion), 120.0 (C, counterion), 127.9 (CH, pyridinium ring), 130.4 (CH, counterion), 132.1 (CH, counterion), 143.6 (CH, pyridinium ring), 162.2 (C, pyridinium ring), 163.0 (COH, counterion), 173.6 (COO^-, counterion) ppm.

Analysis: calculated (0.5 mol% crystal water), 73.89 %C, 9.54 %H, 3.31 %N; found, 73.51 %C, 9.54 %H, 3.20 %N.

1-n-Propyl-4-n-dodecylpyridinium Salicylate (16)

For the ^{1}H–NMR ($CDCl_3$, 200 MHz), δ = 0.82 (6H, t), 1.21 (18H, b), 1.53 (2H, m), 1.86 (2H, m), 2.67 (2H, t), 4.47 (2H, t), 6.66 (2H, m), 7.14 (1H, m), 7.59 (2H, d), 7.81 (1H, d), 8.86 (2H, d) ppm. For the ^{13}C–NMR ($CDCl_3$, 200 MHz), δ = 10.4 (CH_3, 1-alkyl chain), 14.1 (CH_3, 4-alkyl chain), 22.6–35.7 (CH_2, alkyl chain), 62.5 (N^+-CH_2), 116.1 (CH, counterion), 117.1 (CH, counterion), 120.0 (C, counterion), 127.8 (CH, pyridinium ring), 130.4 (CH, counterion), 132.1 (CH, counterion), 143.9 (CH, pyridinium ring), 162.2 (C, pyridinium ring), 163.0 (COH, counterion), 173.7 (COO^-, counterion) ppm.

Analysis: calculated, 75.84 %C, 9.66 %H, 3.28 %N; found, 76.01 %C, 9.71 %H, 3.39 %N.

1-(3-Hydroxy-n-propyl)-4-n-dodecylpyridinium Salicylate (17)

For the ^{1}H–NMR ($CDCl_3$, 200 MHz), δ = 0.89 (3H, t), 1.27 (18H, b), 1.59 (2H, m), 2.20 (2H, m), 2.73 (2H, t), 3.67 (2H, t), 4.87 (2H, t), 6.78 (2H, m), 7.23 (1H, m), 7.60 (2H, m), 7.86 (1H, d), 8.97 (2H, d) ppm. For the ^{13}C–NMR ($CDCl_3$, 200 MHz), δ = 14.1 (CH_3, 4-alkyl chain), 22.6–35.7 (CH_2, alkyl chain), 57.2 (β-CH_2, 1-alkyl chain), 58.6 (N^+-CH_2), 100.0 (CH_2OH), 116.3 (CH, counterion), 117.1 (CH, counterion), 120.0 (C, counterion), 127.6 (CH, pyridinium ring), 130.5 (CH, counterion), 132.5 (CH, counterion), 144.2 (CH, pyridinium ring), 161.9 (C, pyridinium ring), 163.0 (COH, counterion), 172.1 (COO^-, counterion) ppm.

Analysis: calculated (0.5 mol% crystal water), 71.65 %C, 9.35 %H, 3.09 %N; found, 71.98 %C, 9.20 %H, 3.08 %N.

1-Methyl-2-n-dodecylpyridinium Salicylate (18)

For the ^{1}H–NMR ($CDCl_3$, 200 MHz), δ = 0.88 (3H, t), 1.26 (18H, b), 1.65 (2H, m), 2.90 (2H, t), 4.42 (3H, s), 6.68 (2H, m), 7.17 (1H, m), 7.54 (1H, d), 7.76 (2H, d), 8.14 (1H, d), 9.43 (1H, b) ppm. For the ^{13}C–NMR ($CDCl_3$, 200 MHz), δ = 14.1 (CH_3, 4-alkyl chain), 22.7–32.8 (CH_2, alkyl chain), 45.5 (N^+-CH_3), 116.1 (CH, counterion), 117.0 (CH, counterion), 125.8 (C, counterion), 127.0 (CH, pyridinium ring), 130.4 (CH, counterion), 131.9 (CH, counterion), 144.4 (CH, pyridinium ring), 148.0 (CH, pyridinium ring), 158.1 (C, pyridinium ring), 162.2 (COH, counterion), 173.5 (COO^-, counterion) ppm.

Analysis: calculated (1 mol% crystal water), 71.91 %C, 9.41 %H, 3.35 %N; found, 71.91 %C, 8.83 %H, 3.48 %N.

CMC Measurements

Critical micelle concentrations and degrees of counterion binding were determined using conductivity measurements. Conductivities were measured using a Wayne–Kerr Autobalance Universal Bridge B642 fitted with a Philips electrode PW 9512101 with a cell constant of 0.71 cm^{-1}. The solutions were thermostatted in the cell for at least 15 min before measurements were initiated. The conductivity cell was equipped with a magnetic stirring device. The surfactant concentration in the cell was increased by addition (microsyringe) of 30 to 50 μL aliquots of a concentrated surfactant solution to the conductivity medium. Concentrations were corrected for volume changes. CMC values were taken from the intersection of the tangents drawn before and after the break in the conductivity vs concentration plot. The degree of counterion binding is taken as 1 minus the ratio of slopes of the conductivity vs concentration curve above and below the CMC (20).

Titration Microcalorimetry

Enthalpograms were recorded using a Microcal Omega titration microcalorimeter (Microcal, Northampton, MA). All water used was doubly distilled and all solutions were degassed before use. In a typical experiment the main cell and reference cell were totally filled with water (1.3 mL). The syringe contained a surfactant solution having a concentration approximately 20 times the CMC. The sample cell was stirred (350 rpm) to ensure complete mixing. After thermal equilibrium had been achieved, the first aliquot was injected (5–10 μL). The heat absorbed or evolved was recorded, and subsequently the next aliquot was injected after thermal equilibrium was reached (typically 210 s between injections and an injection time of 20 s). This procedure was repeated until the desired concentration range was covered. The raw data were analyzed using Omega software (Origin 2.9).

The difference in enthalpy of dilution below and above the CMC was taken as the enthalpy of micelle formation (21).

Heat capacities of micellization were calculated from the enthalpies of micellization as a function of temperature in the temperature range 30–60°C.

RESULTS AND DISCUSSION

Influence of Counterions on Micellar Growth

The concentration at which a sphere-to-worm transition takes place in aqueous solution is highly dependent on the molecular architecture of the surfactant, and this change in aggregate morphology can be followed using ^{1}H NMR. Motions of spherical micelles in solution are isotropic on the ^{1}H NMR time scale. The motions of the much larger wormlike micelles are slower and anisotropic. The linewidths of all C–H resonances of the surfactants in spherical micelles are rather sharp, whereas the line widths of all C–H resonances of surfactant molecules in wormlike micelles are broad (22). Since these changes in linewidth occur at sphere-to-worm transitions, the critical wormlike micelle concentration (CWMC) can be calculated from a plot of the peak width at half height ($\Delta\nu_{1/2}$) versus the concentration of surfactant (Fig. 1). An S-shaped curve is obtained. The CWMC was identified as the surfactant concentration where micelles started to grow.

The sphere-to-worm transition can also be studied using microcalorimetry. This technique yields the CWMC and the enthalpy change associated with the sphere-to-worm transition. Using this technique, we observed a transition for surfactant **1** at a concentration of 45 m*M* when wormlike micelles (at concentrations far above the CWMC) were injected stepwise into water. This CWMC value agrees with the value (6) obtained using ^{1}H NMR, 45 m*M*. The enthalpy change associated with the sphere-to-worm transition, -0.5 kJ mol^{-1}, is attributed to a further decrease in apolar surface area exposed to water. Because these enthalpies are small, measurements of a CWMC using microcalorimetry can experimentally be difficult.

The influence of counterions on the CWMC of 1-methyl-4-*n*-dodecylpyridinium surfactants is shown in Table 1. It appears that the CWMC is strongly dependent on the nature of

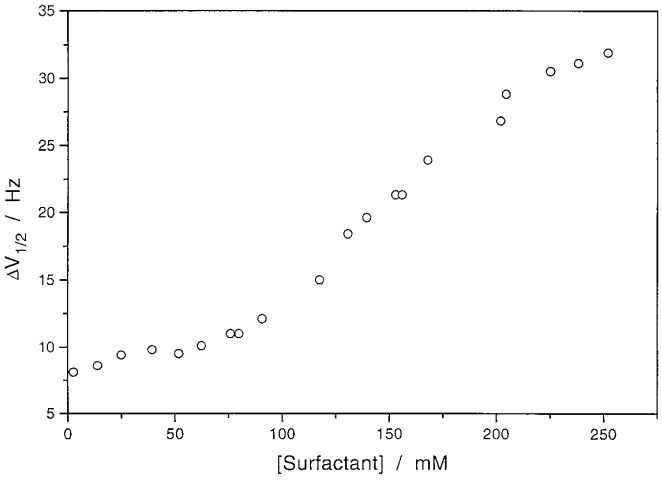

FIG. 1. Line width at peak half height ($\Delta\nu_{1/2}$) of the alkyl chain resonance of surfactant **6** at ca. 1.2 ppm in D_2O as a function of surfactant concentration at 30°C.

the counterion. Changing the counterion from iodide to bromide strongly inhibits micellar growth.

Gamboa *et al.* (16, 23) studied the aggregation behavior of *n*-cetyltrimethylammonium tosylate surfactants in aqueous solution. Spherical micelles are initially formed at a concentration of 0.26 m*M;* these micelles start to grow above the CWMC (15 m*M*).

Previously we have shown that aromatic counterions penetrate between headgroups (19). These surfactants usually have a high degree of counterion binding and aromatic counterions may display favorable interactions with the pyridinium headgroups. As a result, the optimal headgroup area is smaller, compared to bromide, and these surfactants are able to undergo sphere-to-worm transitions at relatively low concentrations. This is reflected in the relatively low CWMC for surfactant **3.** A methyl substituent in the *para* position (**4**) results in a lower CMC (19), a higher degree of counterion binding, and a stronger tendency to grow, because interactions between the counterion and surfactant headgroup are enhanced. Gamboa *et al.* (16) examined the influence of counterions on the viscosity of solutions containing cetyltrimethylammonium salts (CTA salts) and reported that strongly bound counterions produce a more dramatic increase in relative viscosity.

Tosylate and benzenesulphonate counterions are bound more strongly (24) than, for example, bromide at the micellar surface as a result of both electrostatic and hydrophobic interactions with the headgroup. A relative viscosity of 7.000 is recorded (16) for the CTAB/$NaNO_3$ system, whereas the relative viscosity is 100.000 for the same cationic surfactant in the presence of added sodium tosylate. Furthermore, tosylate is more effective than benzenesulfonate in increasing the relative viscosities of CTA salts. These data are in accordance with the measurements reported in this paper: tosylate is also more effective than benzenesulfonate in inducing the sphere-to-worm transition of alkylpyridinium surfactants.

Counterion binding increases (19) on going from surfactant **5** to **3** to **4,** in which the substituent in the counterion is hydrophilic for **5** and hydrophobic for **4,** suggesting a link between hydrophobicity and the degree of counterion binding. The CWMC values, however, do not follow this trend. This means that besides electrostatic interactions other interactions must play an important role in determining the micellar growth. The difference in CWMC between **3** and **4** is explained on the basis of enhanced hydrophobic interactions between counterion and surfactant monomer in the aggregate. The relatively low CWMC for surfactant **5** cannot be explained on the basis of either electrostatic interactions or hydrophobicity. Assuming that wormlike micelles still have an appreciable degree of water penetration (19), interactions between the hydroxy group and water presumably promotes micellar growth relative to surfactant **3.** The same trend is seen when surfactants **6** and **7** are compared. The hydroxy–water interactions seem to be more pronounced in the process of micellar growth than in the process of micellization, since the CMC values and degrees of counterion binding only show small differences (19) for surfactants **6** and **7.**

A hydroxy substituent at the *meta* position (surfactant **8**) experiences a favorable microenvironment (the hydroxy group now points into the Stern layer). Although hydroxy–solvent interactions are enhanced, each counterion is "tilted" with respect to the surfactant monomer. Counterion–solvent interactions tend to decrease optimal headgroup areas, whereas a "tilted" orientation of counterions increases the optimal headgroup areas. For surfactants **7** and **8** these factors balance, and wormlike micelles start to form at about the same concentration. Underwood and Anacker (25) reported aggregation numbers for decyltrimethylammonium micelles with substituted benzoate counterions. The micelle with benzoate as counterion has an aggregation number of 53, with *p*-hydroxybenzoate 48, and with *m*-hydroxybenzoate 68. These different aggregation

TABLE 1

Influence of Counterions on the Sphere-to-Worm Transition of 1-Methyl-4-n-dodecylpyridinium Surfactants in D_2O at 30°C

Surfactant	Aggregate morphology[a]	CWMC (m*M*)	CWMC/CMC
1	M–SM–WM	45[b]	18[b]
2	M–SM–WM	ca. 600[b]	ca. 121[b]
3	M–SM–WM	40	20
4	M–SM–WM	9	6
5	M–SM–WM	29	13
6	M–SM–WM	40	17
7	M–SM–WM	19, 22[c]	7
8	M–SM–WM	19	10
9	M–WM	0.7	—[d]

[a] WM, wormlike micelles; SM, spherical micelles; M, monomers.
[b] According to Ref. (5).
[c] Measured using microcalorimetry.
[d] No indication of the presence of spherical micelles was found.

numbers most likely point to differences in microenvironments of the counterions which have an influence on the interactions determining micellization and micellar growth.

Wormlike micelles start to grow in very dilute solutions for surfactant **9.** Salicylate ions orient parallel to the surfactant monomer and hydroxy groups consequently experience favorable environments. With hydroxy groups in the *ortho* position, there is a distinct hydrophobic part in the counterion, comprising the larger part of the aromatic ring, and a narrow hydrophilic part comprising the carboxylate group and the hydroxy group in close proximity. Such a division, as well as the hydrogen bonding stabilization at the micellar interface, is absent for the other hydroxybenzoate counterions. Lin *et al.* (26) already stressed the importance of such a division in hydrophobic and hydrophilic regions in the formation of wormlike micelles for a solution containing nearly equal amounts of cetyltrimethylammonium bromide and sodium salicylate.

Influence of the Molecular Architecture of Surfactant Monomers on the Formation of Entangled Networks of Wormlike Micelles by Alkylpyridinium Salicylate Surfactants: The Critical Wormlike Micelle Concentration

Salicylate ions are most effective in facilitating micellar growth; extremely long wormlike micelles may be formed in very dilute solutions. Previously we have shown that next to electrostatic interactions, hydrophobic interactions and counterion–solvent interactions play the most important role (19). This section describes a study of the structural requirements of the surfactant (cationic) monomers necessary to induce this unusual micellar growth.

The influence of molecular architecture of surfactant monomers on the CWMC and the degree of counterion binding for alkylpyridinium salicylate surfactants are reported in Table 2.

^{1}H NMR spectra in D_2O, at a concentration of twice the CMC, revealed sharp peaks for surfactant **12,** whereas relatively broad peaks were observed for the other surfactants reported in Table 2. The present results indicate that surfactant **12** aggregates in spherical micelles above the CMC, whereas the other surfactants form wormlike micellar structures under similar conditions. Surfactant **9** has the most pronounced aggregation behavior and forms extremely long, wormlike micelles upon aggregation (solutions just above the CWMC for this surfactant are viscoelastic). This remarkable growth is absent for surfactants **11** and **13–18,** which probably first form wormlike micelles of moderate length (where no viscoelasticity is observed). At higher concentrations these wormlike micelles grow and may form a network of entangled wormlike micelles, depending on the molecular architecture of the surfactant monomer. Using ^{1}H NMR line-broadening experiments, it was found that spherical micelles formed by surfactant **12** start to grow at a concentration of 4 m*M* (at 30°C) to form wormlike micelles of moderate length.

TABLE 2

Influence of Molecular Architecture on the CWMC and Counterion Binding of Alkylpyridinium Salicylate Surfactants at 30°C

Surfactant	CWMC (m*M*)	β (%)
9	0.7	87
11	3.4	93
12	1.8[a]	93
13	0.4	75
14	0.1	71
15	0.7	82
16	0.6	83
17	0.8	82
18	1.2	89

[a] This surfactant forms more or less spherical micelles.

Decreasing the length of the hydrophobic moiety of the surfactant (**9** vs **11**) results in an increase in the CWMC by about a factor of 2 per methylene group. The same trend and value is found when surfactants **12, 13,** and **14** are compared.

Nusselder *et al.* (6, 27) studied the aggregation behavior of 1-alkyl-4-n-dodecylpyridinium iodide surfactants in water at 30°C. The CMC and CWMC decrease upon increasing headgroup hydrophobicity. This pattern was attributed to favorable London dispersion interactions between the 1-alkyl chains. This favorable interaction is counteracted by a decrease in hydration of the headgroup region. As far as the stability of the aggregate is concerned, the first effect is dominant and the CMC decreases, and hence the Gibbs energy of micelle formation decreases.

As is shown in Table 2, the influence of headgroup hydrophobicity on the CWMC (**9** and **15–17**) is only moderate. This suggests that the gain in 1-alkyl chain interactions is nearly balanced by the decrease in counterion–water interactions. When iodide is compared with salicylate as counterion, the difference in aggregation behavior (i.e., CMC as a function of headgroup hydrophobicity) appears to be related to the hydrophobicity of the microenvironment of the counterion. Counterion hydration appears to play a much stronger role in the aggregation behavior of surfactants with salicylate counterions than with iodide counterions.

The higher CWMC of **18,** as compared with that of **9,** is attributed to the unsymmetric nature of the surfactant monomer **18.** Nusselder *et al.* (27) studied the effect on the CMC and CWMC of changing the alkyl chain from the 4- to the 2-position in the pyridinium ring for 1-methyl-*x*-dodecylpyridinium iodide surfactants. The concentration at which wormlike micelles are formed is higher for the unsymmetric surfactant than for the symmetric one. On the basis of packing constraints and headgroup areas, a higher CWMC for **18** would be anticipated, when compared to **9.**

Enthalpies of Micellization

Surfactant **9** apparently forms the most "structured" aggregates. The surfactant monomers pack closely, and electrostatic headgroup repulsions are mitigated by a high degree of counterion binding. The hydrocarbon–water contact is strongly reduced upon micellization. The counterion has electrostatic and hydrophobic interactions with the surfactant monomers in the micelles, and the counterion has favorable interactions with the solvent. Also, the distinct hydrophobic–hydrophilic separation of regions in the counterion contributes to an favorable enthalpic contribution to micellization. That surfactant **9** possesses the most exothermic enthalpy of micellization for all surfactants studied in this paper can be understood in these terms. (See Table 3).

As anticipated, a decrease in hydrocarbon chain length results in a less exothermic enthalpy of micellization (compare **9** with **11** and **12–14**). Previously we have shown that the enthalpy of micellization was unaffected by the headgroup hydrophobicity of 1-alkyl-4-*n*-dodecylpyridinium iodide surfactants, although the Gibbs energy of micellization decreases upon increasing headgroup hydrophobicity (19). However, when headgroup hydrophobicity increases (**9, 15,** and **16**), enthalpies of micellization become less exothermic for 1-alkyl-4-*n*-dodecylpyridinium salicylate surfactants. This trend reveals the importance of the microenvironment of the counterions. A hydrophobic environment results in less favorable counterion hydration, which leads to a less exothermic enthalpy of micellization. This trend again highlights the importance of counterion–water interactions for the aggregation behavior of alkylpyridinium salicylate surfactants. Surfactant **17** has a relatively hydrophilic 1-alkyl chain and a relatively exothermic enthalpy of micellization. The hydrophobicity of the 1-alkyl chain, expressed as the sum of Rekker's (29) hydrophobic fragmental constants (Σf_i), is 1.232 for ethyl, 1.762 for *n*-propyl, and 0.099 for 3-hydroxy-*n*-propyl. The less symmetric nature of surfactant **18** results in less exothermic enthalpies of micellization.

TABLE 3

Enthalpies of Micellization (in kJ mol^{-1}) at Different Temperatures as a Function of Surfactant Structure for Alkylpyridinium Salicylate Surfactants

	T (°C)			
Surfactant	30	40	50	60
9	−22.4	−28.1	−33.8	−38.1
11	−17.8	−22.6	−26.9	−30.8
12	−17.4	−22.5	−27.7	−31.6
13	−18.6	−23.8	−29.8	−34.7
14	−20.9	−27.0	−33.7	−37.9
15	−19.4	−22.5	−28.4	−31.4
16	−17.4	−23.7	−28.8	−32.9
17	−20.3	−25.8	−30.0	−33.2
18	−18.2	−22.5	−29.1	−31.4

TABLE 4

Heat Capacities of Micellization as a Function of Surfactant Structure for Alkylpyridinium Salicylate Surfactants

Surfactant	$\Delta_{mic}C_p^o$ (J mol^{-1} K^{-1})
9	−533
11	−436
12	−476
13	−544
14	−574
15	−407
16	−513
17	−429
18	−462

Heat Capacities of Micellization

The heat capacity of micellization mainly reflects the effect of hydrophobic interactions on the micellization process. When the chain length of the alkyl group of the surfactant increases, the heat capacity of micellization becomes more negative.

Although the differences are small, this trend is also observed for alkylpyridinium salicylate surfactants. When surfactants **9** and **11** are compared, a change in heat capacity of micellization of about −50 J mol^{-1} K^{-1} per methylene group is calculated. A value of −25 J mol^{-1} K^{-1} per CH_2 group is obtained for surfactants **12–14.** Heat capacities of micellization for a series of alkyltrimethylammonium bromide surfactants in aqueous solution (27) are −302 J mol^{-1} K^{-1} for decyl-, −406 J mol^{-1} K^{-1} for dodecyl-, −499 J mol^{-1} K^{-1} for tetradecyl-, and −573 J mol^{-1} K^{-1} for hexadecyltrimethylammonium bromide in aqueous solution. This decrease in heat capacity of about −45 J mol^{-1} K^{-1} per CH_2 group is in pleasing accordance with our data. (See Table 4).

No trend in heat capacity of micelle formation as a function of headgroup hydrophobicity is observed. However, surfactants **15–17** reveal that more hydrophobic headgroups (e.g., containing 1-alkyl chains) yield more negative heat capacities of micellization. The fact that surfactant **9** does not fit into this series could be due to the fact that this surfactant forms long, wormlike micelles. This results in a more efficient and stronger reduction of the apolar hydrocarbon chain–water contact, thereby making the heat capacity of micellization more negative.

Formation of Entangled Networks of Wormlike Micelles by Alkylpyridinium Salicylate Surfactants

Interestingly, solutions of cationic surfactants with added sodium salicylate do not always form viscoelastic solutions. This phenomenon depends strongly on the molecular architec-

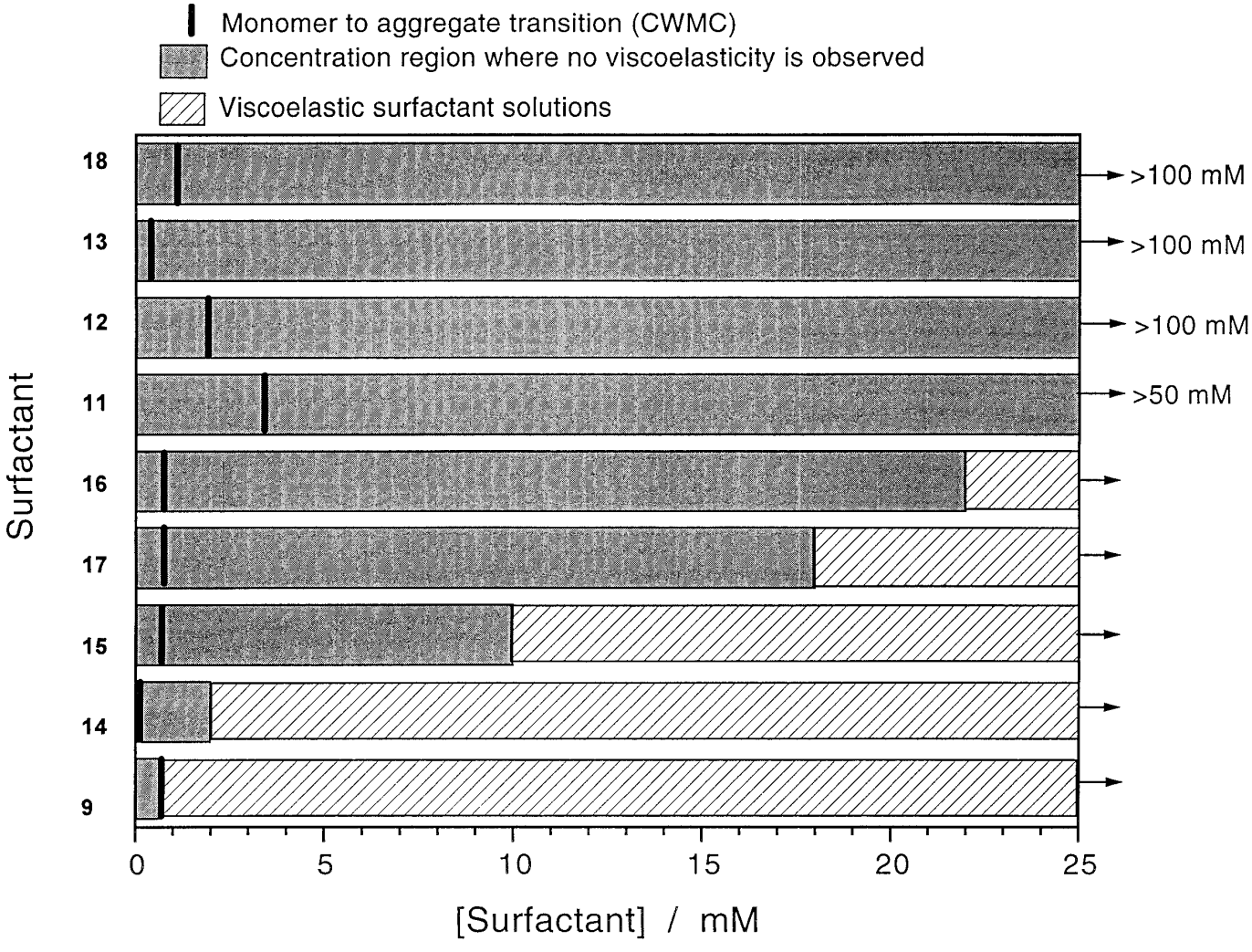

FIG. 2. Concentration at which an entangled network of wormlike micelles is formed at room temperature as a function of surfactant structure.

ture of the surfactant monomer. Figure 2 shows the influence of surfactant structure on the critical concentration where viscoelasticity is first observed. The reported critical entangled wormlike micelles concentration (CEWC) is the concentration where wormlike micelles start to overlap and entangle. Viscoelasticity is revealed by swirling a surfactant solution of a given concentration and visually observing the recoil of trapped air bubbles. The solution was diluted stepwise and the minimum concentration for viscoelasticity was determined. The solutions were allowed to equilibrate for two days and the experiment was repeated. Dilution was repeated to a concentration at which viscoelasticity had disappeared.

As can be seen in Fig. 2, surfactant **9** induces the formation of an entangled network of wormlike micelles at concentrations directly above the CWMC. Increasing headgroup size results in a strong increase in the CEWC, and in fact no viscoelasticity could be detected up to a concentration of 100 m*M* for surfactant **12.**

Increasing the chain length in the 1-*n*-alkyl-4-methylpyridinium salicylate surfactants lowers the CEWC. Surfactant **14** forms an entangled network of wormlike micelles at 2.0 m*M*, which is 20 times the CWMC. Increasing the chain length of the alkyl group results in stronger interactions between the surfactant monomers favoring the formation of larger aggregates. The CEWC for surfactant **14** was observed visually, and also using titration microcalorimetry. Upon injection of a concentrated surfactant solution of surfactant **14** into water, a large exothermic monomer-to-wormlike micelle transition was observed at 0.1 m*M*. Upon increasing the concentration of surfactant in the sample cell, a second endothermic transition was observed at 2.0 m*M*. The enthalpy change associated with this process (ca. 1 kJ mol^{-1}) is attributed to the formation of an entangled network of wormlike micelles from unentangled wormlike micelles. Viscoelasticity was observed (see Fig. 2) at concentrations above 2.0 m*M*. Due to this phenomenon the syringe will experience a force opposite to the stirring direction. This force, which arises from the entanglements, results in small irregular heat effects.

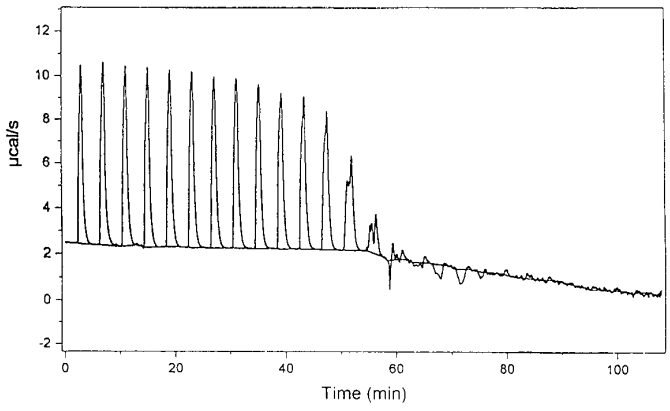

FIG. 3. Titration microcalorimetric output for solutions of surfactant **9.** Baseline instabilities, indicating the presence of an entangled network of wormlike micelles, are observed beyond the CEWC.

Experimentally, baseline instabilities were observed at surfactant concentrations above 2.0 m*M* of surfactant **14.** Baseline instabilities also occur at concentrations above the CEWC for aqueous solutions of surfactant **9** (Fig. 3).

The decrease in CEWC upon increasing headgroup hydrophobicity is further illustrated by ^{1}H NMR experiments, which indicate that the counterions are located between pyridinium headgroups. Quite substantial upfield shifts are found for the pyridinium ring protons, indicating the close approach of the pyridinium headgroups and the aromatic counterions. When headgroup hydrophobicity increases, growth of wormlike micelles is hampered. A more apolar environment affects the counterion hydration and therefore influences the concentration at which an entangled network of wormlike micelles is formed. Hydrogen bonding between counterions and water appears to facilitate the formation of very long, wormlike micelles. In our laboratories (30), the aggregation behavior of surfactant **9** has also been studied in water/urea and water/tetramethylurea mixtures. As expected, the CMC increases with increasing urea or tetramethylurea concentration. Furthermore, the viscoelasticity found for surfactant **9** in water was absent in both 8 *M* urea or 8 *M* tetramethylurea. Recently (31), it was argued that urea molecules are mainly located near headgroups at the micellar surface. These findings substantiate the importance of counterion–water (e.g., hydrogen bonding) interactions.

Besides headgroup hydrophobicity, the 4-alkyl chain length also has a large influence on the CEWC (see Fig. 2). The results for surfactants **9** and **11** reveal a relation between chain length of the hydrophobic moiety and appearance of viscoelasticity. Measurements by Sakaiguchi *et al.* (32) on the aggregation behavior of cetyltrimethylammonium bromide solutions containing equimolar amounts of salicylic acid are in accordance with our findings. These solutions exhibit strong viscoelasticity. Solutions containing equimolar amounts of dodecyltrimethylammonium bromide and salicylic acid are not viscoelastic.

For surfactant **18** no network of entangled wormlike micelles is observed at concentrations below 100 m*M*, although salicylate ions associate strongly at the surface of these micelles. Apparently, the unsymmetric nature of the surfactant inhibits the growth of wormlike micelles because interactions between surfactant monomers are less favorable due to the unsymmetric nature of the molecule. Consequently, the optimal headgroup area is larger as compared to **9.** The minimum requirements for growth of wormlike micelles are not met in dilute solutions, and therefore growth of wormlike micelles is much less pronounced.

Solutions containing 1-methyl-4-*n*-dodecylpyridinium *p*-chlorobenzoate are also viscoelastic at concentrations above 1.2 m*M* (CWMC = 0.7 m*M*). The hydrophobic chloro substituent is in a favorable environment and micellar growth is facilitated, but not as effectively as for salicylate (**9**).

Counterions Which Are Able To Induce Viscoelasticity in Surfactant Solutions

As shown before, the detailed molecular structure of the aromatic counterion affects the formation of a network of entangled wormlike micelles. Below we discuss the role of various aromatic counterions in this process.

Gravsholt (7) reported that cetyltrimethylammonium surfactants form viscoelastic solutions with *o*-hydroxybenzoate (salicylate) as a counterion, whereas solutions with *p*- and *m*-hydroxybenzoate counterions do not. Rather unexpectedly, *o*-chlorobenzoate is ineffective, whereas the *p*- and *m*-chlorobenzoates do form viscoelastic solutions. The anion of methylsalicylic acid is able to induce the formation of a network of wormlike micelles when the methyl substituent is placed on the 3,4, or 5 position (26). Toluates (33) are effective in the formation of very long wormlike micelles when the methyl substituent is *para* or *meta*, but the *o*-toluate-containing surfactant does not form viscoelastic solutions. Brown *et al.* (34) studied the aggregation behavior of cetyltrimethylammonium bromide with added sodium naphthalenesulfonate. At concentrations of 20 m*M* or higher, viscoelasticity was observed, and above 100 m*M* a gel was formed. As shown previously (19), the microenvironment and orientation of counterions are important parameters for micellization and micellar growth. Relatively hydrophobic substituents (chloro or methyl) seem to be most effective when they reside in more hydrophobic parts of the Stern region. When these substituents point out of the Stern region, unfavorable substituent–water interactions hamper micellar growth. The hydroxy group, in contrast, is a hydrophilic substituent; therefore it favors the *ortho* position, because it takes part in hydrogen-bonding interactions with water present in the Stern layer. Headgroup stabilization through hydrogen-bonding interactions between counterions and water further facilitates micellar growth. When the hydroxy substituent is positioned at the meta position, it points out of the Stern region, but its unfavorable orientation (tilting of counterions with respect to the headgroup) prevents a close approach of surfac-

tant monomers and consequently does not favor micellar growth.

Only a limited number of studies are known in which the aromatic counterion is not added as a salt to a cationic surfactant. Gravsholt (7), for example, prepared a series of surfactants with different counterions using an ion exchanger. Frequently, however, studies (25, 34) used commercially available cationic surfactants, e.g., cetyltrimethylammonium bromide, and added sodium salts of the desired counterion.

The latter procedure means that the measurements are in fact performed in mixed aqueous electrolyte solutions. Apart from this, micellization and micellar growth is also dependent on the counterion concentration, when the counterion is added to the surfactant solution. Lin *et al.* (26) studied the aggregation behavior of cetyltrimethylammonium bromide/5-methylsalicylic acid as a function of the molar ratio of surfactant/counterion (C_s/C_c) using cryo-electron microscopy. At a molar ratio of 0.1, only spherical micelles having a diameter of about 60 Å could be detected. At a molar ratio of 0.2, wormlike micelles with the same diameter started to form. At a molar ratio of 0.3, long, wormlike micelles started to form. At molar ratios of 0.4 and 0.5, the wormlike micelles became very long and started to overlap, but there were still spherical micelles coexisting in the solution. When the molar ratio reached 0.7, very few spherical micelles were present and wormlike micelles started to form an entangled network. At a 1.1 molar ratio of 5-methylsalicylic acid and cetyltrimethylammonium bromide, the solution became visibly turbid. Vesicles were observed using cryo-electron microscopy. Cetyltrimethylammomium bromide formed (26) spherical micelles when *p*-hydroxybenzoic acid was added, and short, wormlike micelles coexisting with spherical micelles when *m*-hydroxybenzoic acid was added.

The factors which determine the growth of wormlike micelles to such an extent that they form viscoelastic solutions at extremely low concentration are not understood. Rao *et al.* (35) proposed a micellar chain model. An important parameter is the orientation of the counterion at the micellar surface. A correlation was suggested (35) between this orientation and the worm-inducing efficiency.

The carboxylate moieties of salicylate and *p*-chlorobenzoate ions project out of the micellar surface (18, 35). This condition is claimed to be favorable for the formation of polymer-like chains of spherical micelles linked through counterions. These micellar chains are responsible (18, 35) for the viscoelasticity. Because *m*-hydroxybenzoate counterions have "tilted" orientations, this counterion cannot serve as a bridge between spherical micelles.

Anet disagrees with these views (36). On the basis of NMR relaxation data, he concluded that salicylate ions have very different tumbling motions in mobile and in viscoelastic micellar solutions. Therefore, the suggestion that viscoelastic solutions contain linked spherical micelles is not likely. Ulmius *et al.* (37) suggested that the properties of these solutions are caused by a periodic colloidal structure, formed as a result of the repulsive force between the aggregates. Fuhrop and Helfrich (38) proposed that helical ribbons are formed when cetyltrimethylammonium bromide and salicylic acid are dissolved in water. These ribbons are reported to have a diameter of 12 nm. However, a satisfactory theory which explains the rheological behavior (when viscoelastic solutions are formed at extremely low concentration) of wormlike micellar systems is still lacking (26).

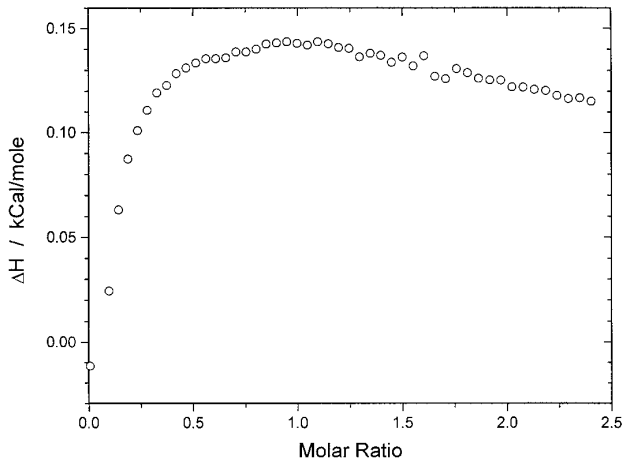

FIG. 4. Titration of sodium bromide into 1-methyl-4-*n*-dodecylpyridinium iodide micelles. Plot of the enthalpy change vs molar ratio, [salt]/[surfactant].

Addition of Salt to Micelles Formed by Cationic Surfactants

Bartet *et al.* (24) studied the association of anions to cationic micelles and explained their results in terms of competition between different anions for binding to micelles. When either tosylate or benzenesulfonate was added to cetyltrimethylammonium bromide micelles, bromide ions were completely displaced by tosylate or benzenesulfonate ions. Tosylate and benzenesulfonate interact with micelles of cetyltrimethylammonium both electrostatically and hydrophobically. Differences in binding between tosylate and benzenesulfonate were found, however. The *p*-methyl group in the tosylate enhances the binding of this anion to the surface of cationic micelles relative to benzenesulfonate. Blandamer *et al.* (39) studied the interaction between dimethyldioctadecylammonium bromide vesicles and sulfate anions in aqueous solution. Results were discussed in terms of two factors: (i) vesicle–dianion interactions which are exothermic and (ii) headgroup dehydration with bromide displacement which is endothermic.

Here we focus on the interaction between anions and cationic micelles. Special emphasis will be put on the interaction between anions which are able to induce the formation of a network of wormlike micelles, e.g., salicylate and *p*-chlorobenzoate, and spherical micelles.

The enthalpy change per mole of added salt as a function of the molar ratio upon titration of sodium bromide to 1-methyl-4-*n*-dodecylpyridinium iodide micelles is shown in Fig. 4. The

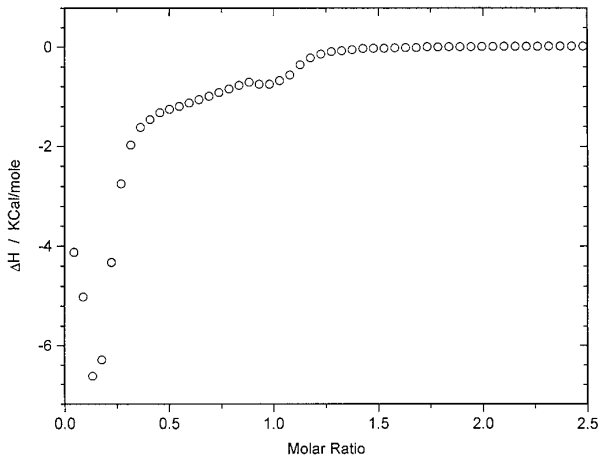

FIG. 5. Titration of sodium salicylate into 1-methyl-4-*n*-dodecylpyridinium iodide micelles. Plot of the enthalpy change vs molar ratio, [salt]/[surfactant].

heat effects, measured by titration microcalorimetry, are small and result mainly from the dilution of sodium bromide in a micellar solution and the competitive binding between iodide and bromide at the micellar surface. Because iodide ions have a smaller hydrated radius than bromide ions, iodide ions have a stronger interaction with cationic micelles. Displacement of iodide by bromide is only moderately effective and heat effects due to this exchange are small. When a bromide ion displaces an iodide anion from the micellar surface, the bromide ion is partially dehydrated (endothermic), the headgroup repulsions increase (endothermic), and the iodide ions move from the micellar surface to the bulk solution, where they become more strongly hydrated (exothermic). The overall enthalpy change is endothermic, reflecting the fact that displacement of iodide by bromide at the micellar surface is enthalpically unfavorable. Heat effects due to injection of a sodium bromide solution, of the same concentration, into water are small and exothermic. The exothermicity is due to the fact that the thermodynamically nonideal properties are more pronounced in the syringe, as a result of the high salt concentration.

Addition of sodium salicylate to spherical micelles is accompanied by enormously large heat effects. The enthalpogram differs greatly from that for addition of "simple" salts to micelles (compare Figs. 4 and 5).

At low molar ratios (i.e., at low concentrations of sodium salicylate) the observed heat effects are mainly due to the interaction of salicylate ions with the cationic micellar surface. The observed minimum at low molar ratios corresponds to a value which is equal to the degree of counterion dissociation at the micellar surface (which is about 0.18 for iodide (19)). This minimum was also found when sodium salicylate was added to micelles with different degrees of counterion dissociation. Addition of salicylate to 1-methyl-4-n-dodecylpyridinium methylsulfonate micelles yielded an enthalpogram which has similar features. The degree of counterion dissociation of methylsulfonate is about 0.47, and the minimum in the enthalpogram is now located at a molar ratio of about 0.54. 1-Methyl-4-n-dodecylpyridinium benzoate micelles have a degree of counterion dissociation of 0.23; addition of sodium salicylate to these micelles gave a minimum in the enthalpogram at a molar ratio of 0.22.

As salicylate concentration increases the spherical micelles formed by cationic surfactants start to grow (26). At higher molar ratios wormlike micelles steadily grow and eventually form an entangled network. A plateau in the enthalpogram is observed after a certain size of the wormlike micelles is reached (Fig. 5). Further addition of sodium salicylate leads to a transition having an enthalpy change of about 2–3 kJ mol^{-1}. This transition is observed for addition of sodium salicylate to micelles formed by 1-methyl-4-*n*-dodecylpyridinium iodide, methylsulfonate, and benzoate, and might be due to a micelle-to-bilayer transition. Addition of salicylic acid (SA) to cetyltrimethylammonium bromide (CTAB) results in the formation of vesicles when the molar ratio (SA/CTAB) exceeds unity (26).

Addition of *p*-chlorobenzoate to spherical micelles of 1-methyl-4-*n*-dodecylpyridinium iodide surfactants revealed similar enthalpograms. At molar ratios of *p*-chlorobenzoate to 1-methyl-4-n-dodecylpyridinium iodide greater than unity no transition was observed, however. The enthalpograms with large heat effects and characteristic minima are not observed when other hydrophobic counterions (e.g., benzoate) are added to spherical micelles. For example, the heat effects observed upon addition of sodium benzoate to spherical micelles formed by 1-methyl-4-*n*-dodecylpyridinium iodide are smaller by a factor of 50. The observed enthalpograms, with their strong exothermic heat effects and minima, are characteristic for the addition of counterions which induce the formation of a network of wormlike micelles to a solution of spherical micelles.

It has been proposed that upon micellization the *o*-hydroxy group of the salicylate ion could be deprotonated (38). This second deprotonation would strongly influence the micellization of cationic surfactants with salicylate counterions. Therefore, the titration of sodium salicylate to micelles formed by 1-methyl-4-*n*-dodecylpyridinium iodide was also performed as a function of the pH. The pH was varied from 4 to 11. The observed enthalpograms revealed the same features. The observed minimum and enthalpy of transition were in the same order of magnitude, independent of the pH. Our pH-dependent measurements, thus, suggest that the hydroxy group is not deprotonated when cationic surfactant with salicylate counterions are studied in aqueous solution.

CONCLUSIONS

This paper describes a detailed study of the influence of counterions on the unidirectional growth of spherical micelles to form wormlike micelles. It is shown that this growth strongly depends on the type and structure of the counterion.

Counterion size, hydration, and structure (e.g., substitution pattern of the aromatic counterion) all play an important role in the growth of spherical micelles to form wormlike micelles. Depending on the molecular architecture of the surfactant cation and (aromatic) counteranion, and on the substitution pattern of the aromatic counterion, extremely long wormlike micelles may be formed. These solutions exhibit viscoelastic behavior. A favorable balance of interactions among the surfactant cation, the counteranion, and the solvent is proposed to be responsible for this phenomenon.

ACKNOWLEDGMENTS

The authors thank The Netherlands Foundation for Chemical Research (SON) and the Netherlands Foundation for Scientific Research (NWO) for their financial support. E.R. thanks the Erasmus Foundation for the travel grant.

REFERENCES

1. Lindman, B., and Wennerström, H., *Top. Curr. Chem.* **87,** 1 (1980).
2. Missels, P. J., Mazer, N. A., Benedek, G. B., and Carey, M. C., *J. Phys. Chem.* **87,** 1264 (1983).
3. Porte, G., Poggi, Y., Appell, J., and Maret, G., *J. Phys. Chem.* **88,** 5713 (1984).
4. Quiron, F., and Magis, L. J., *J. Phys. Chem.* **90,** 5435 (1986).
5. Porte, G., and Appell, J., *in* "Surfactants in Solution" (K. L., Mittal and B. Lindmann, Eds.), Vol. 2, p. 805. Plenum, New York, 1984.
6. Nusselder, J. J. H., Ph. D. Thesis, University of Groningen, 1990.
7. Gravsholt, S., *J. Colloid Interface Sci.* **57,** 575 (1976).
8. Imae, T., Kamiya, R., and Ikeda, S., *J. Colloid Interface Sci.* **108,** 215 (1985).
9. Hayashi, S., and Ikeda, S., *J. Phys. Chem.* **84,** 744 (1980).
10. Ikeda, S., Ozeki, S., and Tsunoda, M., *J. Colloid Interface Sci.* **73,** 27 (1980).
11. Turner, M. S., Margues, C., and Cates, M. E., *Langmuir* **9,** 695 (1993).
12. Clausen, T. M., Vinson, P. K., Minter, J. R., Davis, H. T., Talmon, Y., and Miller, W. G., *J. Phys. Chem.* **96,** 474 (1992).
13. Porte, G., and Appell, J., *J. Phys. Chem.* **85,** 2511 (1981).
14. Ozeki, S., and Ikeda, S., *J. Colloid Interface Sci.* **87,** 424 (1982).
15. Ozeki, S., and Ikeda, S., *J. Colloid Interface Sci.* **77,** 219 (1980).
16. Gamboa, C., and Sepúlveda, L., *J. Colloid Interface Sci.* **113,** 566 (1986).
17. Scheraga, H. A., and Backus, J. K., *J. Am. Chem. Soc.* **73,** 5108 (1951).
18. Manohar, C., Rao, U. R. K., Valaulikar, B. S., and Iyer, R. M., *J. Chem. Soc., Chem. Commun.*, 379 (1986).
19. Bijma, K., and Engberts, J. B. F. N., *Langmuir* **13,** 4843 (1997).
20. Evans, H. C., *J. Chem. Soc.*, 579 (1956); De Lisi, R., Fiscario, E., Milioto, S., *J. Solution Chem.* **17,** 1015 (1988).
21. Bijma, K., Blandamer, M. J., and Engberts, J. B. F. N., *Langmuir* **14,** 79 (1998).
22. Nery, H., Marshal, Y. P., and Canet, D., *J. Colloid Interface Sci.* **77,** 174 (1980).
23. Gamboa, C., and Sepúlveda, L., *J. Phys. Chem.* **93,** 5540 (1989).
24. Bartet, D., Gamboa, C., and Sepúlveda, L., *J. Phys. Chem.* **84,** 272 (1980).
25. Underwood, A. L., and Anacker, E. W., *J. Colloid Interface Sci.* **106,** 86 (1985).
26. Lin, Z., Cai, J. J., Scriven, L. E., and Davis, H. T., *J. Phys. Chem.* **98,** 5984 (1994).
27. Nusselder, J. J. H., and Engberts, J. B. F. N., *J. Org. Chem.* **56,** 5522 (1991).
28. Bashford, M. T., and Woolley, E. M., *J. Phys. Chem.* **89,** 3173 (1985).
29. Rekker, R. F., "The Hydrophobic Fragmental Constant," pp. 350–355. Elsevier, Amsterdam, 1997.
30. Posthumus, W., Engberts, J. B. F. N., and Blandamer, M. J., *J. Mol. Liq.* **73/74,** 91 (1997).
31. Souza, S. M. B., Chaimovich, H., and Politi, M. J., *Langmuir* **11,** 1715 (1995).
32. Sakaiguchi, Y., Shikata, T., Urakami, H., and Hirata, H., *Colloid Polym. Sci.* **265,** 750 (1987).
33. Rehage, H., and Hoffmann, H., *Mol. Phys.* **74,** 933 (1991).
34. Brown, W., Johansson, K., and Almgren, H., *J. Phys. Chem.* **93,** 5888 (1989).
35. Rao, U. R. K., Manohar, C., Valaulikar, B. S., and Iyer, R. M., *J. Phys. Chem.* **91,** 3286 (1987).
36. Anet, F. A. L., *J. Am. Chem. Soc.* **108,** 7102 (1986).
37. Ulmius, J., Wennerström, H., Johansson, L. B. A., Lindblom, G., and Gravsholt, S., *J. Phys. Chem.* **83,** 2232 (1979).
38. Fuhrop, J. H., and Helfrich, W., *Chem. Rev.* **93,** 1565 (1993).
39. Blandamer, M. J., Briggs, B., Butt, M. D., Cullis, P. M., Waters, M., Engberts, J. B. F. N., and Hoekstra, D., *J. Chem. Soc., Faraday Trans.* **90,** 727 (1994).